

# Giant two-photon absorption and its saturation in 2D organic-inorganic perovskite

Liu, Weiwei; Xing, Jun; Zhao, Jiaxin; Wen, Xinglin; Wang, Kai; Lu, Peixiang; Xiong, Qihua

2017

Liu, W., Xing, J., Zhao, J., Wen, X., Wang, K., Lu, P., & Xiong, Q. (2017). Giant two-photon absorption and its saturation in 2D organic-inorganic perovskite. *Advanced Optical Materials*, 5(7), 1601045-. doi:10.1002/adom.201601045

<https://hdl.handle.net/10356/140458>

<https://doi.org/10.1002/adom.201601045>

---

This is the accepted version of the following article: Liu, W., Xing, J., Zhao, J., Wen, X., Wang, K., Lu, P., & Xiong, Q. (2017). Giant two-photon absorption and its saturation in 2D organic-inorganic perovskite. *Advanced Optical Materials*, 5(7), 1601045-, which has been published in final form at <https://doi.org/10.1002/adom.201601045>. This article may be used for non-commercial purposes in accordance with the Wiley Self-Archiving Policy [<https://authorservices.wiley.com/authorresources/Journal-Authors/licensing/self-archiving.html>].

*Downloaded on 13 Mar 2024 19:09:35 SGT*

DOI: 10.1002/adom.

**Article type:** Full Paper

# **Giant Two-photon Absorption and Its Saturation in Two-dimensional Organic-inorganic Perovskite**

*Weiwei Liu, Jun Xing, Jiaxin Zhao, Xinglin Wen, Kai Wang, Peixiang Lu,\* and Qihua Xiong\**

W. Liu, Dr. J. Xing, J. Zhao, Dr. X. Wen, Prof. Q. Xiong  
Division of Physics and Applied Physics, School of Physical and Mathematical Sciences  
Nanyang Technological University  
Singapore 637371

E-mail: [Qihua@ntu.edu.sg](mailto:Qihua@ntu.edu.sg)

W. Liu, Dr. K. Wang, Prof. P. Lu  
Wuhan National Laboratory for Optoelectronics and School of Physics  
Huazhong University of Science and Technology  
Wuhan 430074, China

E-mail: [lupeixiang@hust.edu.cn](mailto:lupeixiang@hust.edu.cn)

Prof. P. Lu

Laboratory of Optical Information Technology  
Wuhan Institute of Technology  
Wuhan 430205, China

**Keywords:** 2D organic-inorganic perovskite; multi-quantum-well structure; nonlinear optics; optoelectronic devices; two-photon absorption

## **Abstract**

Organic-inorganic perovskites have attracted great attentions driven by exceptional progress in photovoltaics, photonics and optoelectronics. Different from the corner sharing framework of three-dimensional (3D) perovskite, two-dimensional (2D) organic-inorganic perovskites possess a layered staking structure composed of alternative organic and inorganic components. Due to the inherent multi-quantum-well-like structure, it is intriguing to explore the optical properties of 2D perovskites enabled by spatial and dielectric confinement. Herein, the two-photon absorption (TPA) properties of 2D perovskite phenylethylamine lead iodide ((PEA)<sub>2</sub>PbI<sub>4</sub>) are systematically studied. The 2D perovskite exhibits a giant TPA and saturation effect under excitation of 800 nm femtosecond laser. The TPA coefficient of a (PEA)<sub>2</sub>PbI<sub>4</sub> flake is measured to be about 211.5 cm/MW, which is at least one order of magnitude larger than those of 3D perovskite films and some typical semiconductor

nanostructures. The giant TPA can be attributed to the enhanced quantum and dielectric confinement in the organic-inorganic multi-quantum-well structure. In addition, a highly thickness-dependent TPA is observed for the 2D perovskite flakes. The result advocates a great promise of 2D organic-inorganic perovskites for nonlinear optical absorption related optoelectronic devices.

## **1. Introduction**

Organic-inorganic hybrid perovskites, composed of alternative stacking sheet of organic and inorganic components, have attracted great attentions due to their unique optoelectronic properties.<sup>[1, 2]</sup> Previous studies show that perovskites have a low defect density,<sup>[3]</sup> a long carrier diffusion<sup>[4]</sup> and a large linear absorption at the band edge,<sup>[5]</sup> making them promising for applications in high-efficiency solar cells,<sup>[5, 6]</sup> high-brightness light-emitting diodes,<sup>[7, 8]</sup> low-threshold optically pumped nanolasers<sup>[3, 9, 10]</sup> and high-performance laser cooling devices.<sup>[11]</sup> Recently, two-dimensional (2D) organic-inorganic hybrid perovskites, which possess a layered staking structure composed of alternative organic and inorganic components, are emerging as promising candidates for nanophotonics and optoelectronics.<sup>[12, 13]</sup> Compared with the typical semiconductors and 3D perovskites, 2D perovskites were demonstrated to possess some outstanding characteristics such as stronger quantum confinement and greater tunability.<sup>[13, 14]</sup> Because of that, the study of 2D perovskites has opened up opportunities for fundamental research and practical applications on a new territory of functional optoelectronic devices based on 2D perovskites.<sup>[11, 15, 16]</sup>

The nonlinear optical properties of nanomaterials play important roles for studying the light-matter interaction and revealing the ultrafast dynamics.<sup>[17-19]</sup> In particular, there has been great interest in nonlinear absorption because of the general applicability for various materials such as semiconductors,<sup>[20, 21]</sup> metal particles<sup>[22]</sup> and synthetic resins.<sup>[23]</sup> 3D perovskites with centrosymmetric structures, have become a new family of good candidates that exhibit large

nonlinear absorption and show great potentials for nonlinear optical devices. For example, the bulk crystal of  $\text{CH}_3\text{NH}_3\text{PbBr}_3$  ( $\text{MAPbBr}_3$ ) was demonstrated as two-photon perovskite photodetectors.<sup>[24]</sup> Also, the  $\text{MAI}_{3-x}\text{Cl}_x$  films were reported to exhibit nonlinear optical response and present a promising application as optical modulators.<sup>[25]</sup> More recently, the nonlinear absorption properties of  $\text{MAPbBr}_3$  and  $\text{CsPbBr}_3$  colloidal quantum dots were studied to compare their differences.<sup>[26]</sup> Concerning 2D perovskites with unique layered stacking structure, it has shown significant importance to investigate their nonlinear absorption properties for further study and practical applications.

Herein, we perform a systematic study on the TPA properties of the 2D organic-inorganic perovskites. The results show that the 2D perovskite  $(\text{PEA})_2\text{PbI}_4$  exhibits a giant TPA for femtosecond pulses at 800 nm, accompanying with a TPA saturation effect. The TPA coefficient for a  $(\text{PEA})_2\text{PbI}_4$  flake with  $\sim 1$   $\mu\text{m}$  thickness is determined to be 211.5 cm/MW, which is at least one order of magnitude larger than those of 3D perovskites and some typical semiconductor nanostructures. Furthermore, a strong dependence of the TPA coefficient on sample thickness is demonstrated for the 2D perovskite flakes.

## 2. Results and Discussion

Bulk crystals of  $(\text{PEA})_2\text{PbI}_4$  were synthesized by super-saturation precipitation method. After that, layered 2D perovskites flakes were prepared by mechanical exfoliating the bulk crystals using a scotch tape method and transferring onto sapphire substrates. For comparison, the films of  $(\text{PEA})_2\text{PbI}_4$  and 3D perovskite  $\text{MAPbX}_3$  ( $\text{X} = \text{I}, \text{Br}$ ) were also prepared by spin-coating method (detailed in Supporting Information). **Figure 1a** and **b** show the optical microscopy image and the corresponding fluorescence microscope image (excited by a broadband blue light) for one of the prepared  $(\text{PEA})_2\text{PbI}_4$  flakes respectively. The images show that the size of the 2D perovskite flake is over several hundred micrometers. The homogenous surface indicates a good quality of the flake for optical measurement, which is

also confirmed by the bright green emission. Figure 1c shows the XRD pattern of a (PEA)<sub>2</sub>PbI<sub>4</sub> bulk crystal and the well-defined diffraction peaks are corresponding to the (00*h*) series of reflections, indicating the good crystallinity and the high degree of preferred orientation. By tilted scanning electron microscopy (SEM) measurement, the thickness of the flake was determined to be 0.94 μm. The (PEA)<sub>2</sub>PbI<sub>4</sub> flake was further characterized by absorption and photoluminescence (PL) spectra, as shown in Figure 1(d). The absorption spectrum exhibits an absorption edge at 530 nm, corresponding to the bandgap of 2.34 eV. The arrow indicates a negligible linear absorption (absorption coefficient  $1.9 \times 10^3 \text{ m}^{-1}$ ) of the (PEA)<sub>2</sub>PbI<sub>4</sub> flake at 800 nm. The PL spectrum was measured with 800 nm femtosecond laser excitation (black dots). The sharp and narrow peak at about 535 nm (2.32 eV) can be attributed to two-photon absorption induced PL (TPL) because the bandgap of (PEA)<sub>2</sub>PbI<sub>4</sub> is larger than the energy of one photon (1.55 eV) but smaller than two times of the photon energy (3.1 eV). The experimental data can be well fitted with the Lorentz lineshape (green curve), indicating a homogeneous broadening mechanism in the 2D perovskite. More importantly, the strong TPL emission already suggests a large TPA effect of the 2D perovskite flake.

The open aperture (OA) Z-scan technique is the most widely used method to determine nonlinear absorption by measuring the transmittance in the far field.<sup>[27]</sup> The measurement was performed by using a Ti:sapphire femtosecond laser system with regenerative amplifier (Spectra-Physics, 800 nm, 100 fs, 1 kHz). Details on configuration of the set-up are presented in Supporting Information. **Figure 2a** show the typical OA Z-scan results for the (PEA)<sub>2</sub>PbI<sub>4</sub> flake on sapphire substrate. The nonlinear absorption of the substrate is negligible because no noticeable variation can be observed from the Z-scan result of the substrate. For the (PEA)<sub>2</sub>PbI<sub>4</sub> flake, the Z-scan results show that the normalized transmission decreases as the sample approaches to the beam waist ( $z = 0$ ), which is a characteristic feature of TPA effect

that the material absorption increases with the optical intensity. However, the largely reduced transmission at even low optical intensity ( $0.044 \text{ GW/cm}^2$ ) indicates a strong linear scattering. The scattering changes with the variation of the spot size as the sample scans along z-axis,<sup>[24]</sup> resulting in a nonlinear variation of the transmission, which prevents us extracting the TPA coefficient by directly fitting the Z-scan curves. To accurately determine the TPA coefficient, we performed the static intensity-dependent transmission measurement instead, in which the sample was kept at the laser beam waist and the nonlinear transmission was obtained by monitoring the incident and transmitted intensity simultaneously. This method has been proved to be more straightforward and effective by the previous reports.<sup>[24, 28]</sup> Figure 2b shows the intensity-dependent result for the  $(\text{PEA})_2\text{PbI}_4$  flake. The inverse transmission increases gradually as the incident intensity (pumping power) increases, which presents a typical feature for TPA. At low optical intensity (nearly to be zero), there still exists a background (green dashed line), which indicates the linear transmission of the femtosecond laser beam.<sup>[24]</sup>

Two-photon absorption is a third-order nonlinear process that the electrons in the valence band can absorb two photons at the same time and transmit to the conduction band, as illustrated in Figure 2c. For degenerated TPA, the light attenuation in the material can be described as<sup>[24]</sup>

$$\frac{dI(z)}{dz} = -\alpha_0 I(z) - \beta I(z)^2 \quad (1)$$

where  $I(z)$  is the peak intensity within the sample and  $z$  is the propagation distance in the sample.  $\alpha_0$  is the linear absorption coefficient and  $\beta$  is the TPA coefficient of the material. The normalized transmission through the sample can be extracted from the solution of Equation (1), and expressed as<sup>[24, 28]</sup>

$$T(I) = \frac{e^{-\alpha_0 L}}{\beta I L_{\text{eff}} + 1} \quad (2)$$

where  $I$  is the incident intensity, and  $L_{\text{eff}}$  is the effective length of the sample,  $L_{\text{eff}} = [1 - \exp(-\alpha_0 L)]/\alpha_0$ . Considering the reduction by possible reflection and scattering when light passes the sample, a more accurate expression for the normalized transmission will be<sup>[28]</sup>

$$T(I) = \frac{(1-R)^2 e^{-\alpha_0 L}}{(1-R)\beta I L_{\text{eff}} + 1} \quad (3)$$

where  $R$  represents the reduction factor caused by the reflection and scattering. Figure 2b shows that the linear increase of inverse transmission at low incident intensities is in accordance with the theoretical model expressed by Equation (3), which further confirms the TPA process mentioned above. As the incident intensity further increases, the transmission of the (PEA)<sub>2</sub>PbI<sub>4</sub> flake tends to be stable, indicating the saturation of the TPA. In the homogeneously broadened system, the saturated TPA coefficient can be expressed by<sup>[29]</sup>

$$\beta(I) = \frac{\beta_0}{1 + (I / I_{\text{sa}})^2} \quad (4)$$

where  $\beta_0$  is the nonsaturation TPA coefficient, and  $I_{\text{sa}}$  is the saturable intensity. To obtain the TPA coefficients for the 2D perovskite flakes, the experimental data in Figure 2b is fitted with the TPA saturation model expressed by Equation (3) combined with Equation (4) (red curve). For comparison, the result fitted with TPA nonsaturation model (Equation (3)) is also presented (blue dashed line). It can be observed that the experimental data can be fitted well with the TPA saturation model. The fitted result shows that the TPA coefficient  $\beta_0$  is about 211.5 cm/MW for the (PEA)<sub>2</sub>PbI<sub>4</sub> flake. Correspondingly, the TPA saturation intensity is estimated to be 0.21 GW/cm<sup>2</sup>.

The stability of perovskites under intense excitation has become a serious concern for practical applications.<sup>[30]</sup> In the experiment, the stability of the samples was tested by keeping the samples at the focus of the laser beam and recording the transmitted power synchronously. The peak intensity was set to be 0.2 GW/cm<sup>2</sup>, which is much lower than the damage threshold

of the (PEA)<sub>2</sub>PbI<sub>4</sub> flake (0.93 GW/cm<sup>2</sup>, refer to Supporting Information) to protect the sample from being damaged. Figure 2d shows the normalized transmission for a (PEA)<sub>2</sub>PbI<sub>4</sub> flake. It can be observed that for a time period more than 10 minutes, the measured transmission keeps to be a constant, indicating a good stability of the sample during the measurement. In order to investigate the influence of material structure, the TPA property of a (PEA)<sub>2</sub>PbI<sub>4</sub> film was also measured and compared with the flake (refer to Supporting Information). The result shows that the (PEA)<sub>2</sub>PbI<sub>4</sub> film also exhibits a TPA saturation effect under the 800 nm femtosecond laser. By fitting the experimental result with the TPA saturation model, the TPA coefficient and saturation intensity are determined to be 12.6 cm/MW and 0.22 GW/cm<sup>2</sup> respectively. The TPA coefficient of the film is much smaller than that of the (PEA)<sub>2</sub>PbI<sub>4</sub> flake. As the nonlinear absorption of the samples could be sensitively affected by the inhomogeneity and defects of the crystals, the larger TPA indicates a better crystal quality and a more suitable candidate of the 2D perovskite flake for nonlinear optical study and applications.

To reveal the differences between 2D and 3D perovskites, the nonlinear absorption properties of the 3D perovskite (MAPbX<sub>3</sub>, X = I, Br) films were studied as well. **Figure 3a** shows the Atomic Force Microscope (AFM) pattern of a prepared MAPbI<sub>3</sub> film, which exhibits a smooth surface of the film with thickness of about 1 μm. Figure 3b shows the linear absorption spectrum of the MAPbI<sub>3</sub> film. The absorption edge of the MAPbI<sub>3</sub> film is located at about 785 nm. At 800 nm, there still exists an absorption tail so that a considerable single-photon absorption is possible. From the data, the linear absorption coefficient of the MAPbI<sub>3</sub> film is estimated to be  $1.5 \times 10^5 \text{ m}^{-1}$ . Under intense femtosecond pulses, the conduction band states can be populated by the single-photon absorption. Consequently, the inverse transmission versus incident intensity exhibits a saturable absorption property, in which the transmission increases with the optical intensity and tends to be stable, as shown in Figure 3c.

By fitting with the saturable absorption model (red curve), SA coefficient for the MAPbI<sub>3</sub> film can be determined to be -13.6 cm/MW, and the saturable intensity is about 0.4 GW/cm<sup>2</sup>. It should be noted that the measured SA coefficient of the MAPbI<sub>3</sub> film at 800 nm is in the same order as that reported at 532 nm (-152 cm/MW) and 1064 nm (-2.25 cm/MW).<sup>[25]</sup> Figure 3d presents the AFM pattern of a MAPbBr<sub>3</sub> film, showing the film thickness is about 385 nm. The linear absorption spectrum shown in Figure 3e indicates that the absorption edge is at about 520 nm, with a little linear absorption at 800 nm (absorption coefficient  $4.5 \times 10^4 \text{ m}^{-1}$ ). The plot of inverse transmission *versus* incident intensity in Figure 3f shows that the MAPbBr<sub>3</sub> film has a similar TPA saturation property at 800 nm. By fitting, the TPA coefficient is determined to be 5.5 cm/MW.

**Table 1** summarizes the nonlinear absorption parameters of different nanostructures including II-VI semiconductors nanocrystals,<sup>[31, 32]</sup> 2D transition metal dichalcogenide mono/few-layers,<sup>[33]</sup> 2D perovskite flake and 2D/3D perovskite films at 800 nm. All of these nanomaterials are considered to possess remarkable nonlinear optical absorption effects. Among all of them, the nonlinear absorption coefficients of perovskites are overall several orders of magnitude larger than the other materials. In particular, the 2D perovskite (PEA)<sub>2</sub>PbI<sub>4</sub> has the largest TPA coefficient and the value is even one order of magnitude larger than those of the 3D perovskite films. Considering the differences between these materials, the giant TPA of 2D perovskites may originate from the unique layered stacking structure. **Figure 4a** and **b** show the crystalline (left panel) and electronic (right panel) structure of 2D and 3D perovskites respectively. It has been well known that the alternative stacking sheet of organic and inorganic components in the 2D organic-inorganic perovskite can be regarded as a multi-quantum-well structure with organic layer being the barrier and inorganic layer being the well: the energy gap of the organic layer is larger than that of the inorganic layer, while the dielectric constant of the organic layer is smaller than the inorganic

layer, as illustrated in Figure 4a.<sup>[34, 35]</sup> Due to the specific quantum and dielectric confinements, the carriers can be strongly confined in the inorganic layer with atomic-layered thickness, and enhanced light-matter interaction can be obtained, such as strong exciton-photon coupling<sup>[14]</sup> and large oscillator strength of exciton transition.<sup>[36]</sup> The two-photon absorption, originated from third-order nonlinear polarization of electrons, can be enhanced by a factor scaled as double multiplication of the oscillator strength enhancement in the quantum well structure,<sup>[37]</sup>

$$\chi_{enhance}^{(3)} \propto (Q_{dim} Q_{loc})^2 \quad (5)$$

where  $\chi_{enhance}^{(3)}$  denotes the enhancement factor of the third-order nonlinear susceptibility.  $Q_{dim}$  and  $Q_{loc}$  describe the enhancements of oscillator strength due to dimensional confinement and localization of excitons, respectively. The oscillator strength per quantum well in the 2D perovskite (PEA)<sub>2</sub>PbI<sub>4</sub> was reported to be  $3.6 \times 10^{13} \text{ cm}^{-2}$ , which is about one order of magnitude larger than that of the conventional semiconductor quantum well.<sup>[38, 39]</sup> Equation (5) indicates that the TPA coefficient of 2D perovskite flakes can be enhanced by several orders of magnitude compared with the other nanostructures, which is in accordance with the results presented in Table 1. In addition, it was reported that organic molecules could provide greater charge separation and larger transition dipole moment upon excitation,<sup>[26]</sup> which may also have contributed to enhancing the nonlinear absorption properties of the organic-inorganic perovskites.

The layered structure of 2D perovskites makes it convenient to prepare samples with various thicknesses and study the thickness-dependent optical properties. The TPA coefficients of (PEA)<sub>2</sub>PbI<sub>4</sub> flakes with different thicknesses were measured. To make sure that the flakes can cover the whole laser spot, the lateral sizes of the flakes were selected to be larger than the beam waist at focus. The results are presented in **Figure 5** (black stars). It can be observed that the TPA coefficient decreases as the sample thickness increases. This

thickness dependent TPA property can be attributed to the light absorption by the sample (self-absorption). As the laser beam propagates along the sample, the optical intensity will reduce gradually due to the linear absorption and two-photon absorption of the sample, which in return results in a reduced nonlinear absorption. As a result, the measured TPA coefficient becomes reduced as the sample thickness increases. It can be also observed that, when the sample thickness is less than about 10  $\mu\text{m}$ , the sample thickness has a great influence on the TPA. As the thickness further increases, the TPA coefficient tends to be equal to that of the bulk material. This thickness dependent TPA property reveals a superior capability of the nanomaterials for nonlinear absorption, which is of particular significance for realizing high-performance applications by selecting proper sizes of the nanomaterials.

### **3. Conclusion**

In conclusion, the TPA properties of the 2D perovskite are systematically studied at 800 nm. The  $(\text{PEA})_2\text{PbI}_4$  flake exhibits a giant TPA effect, accompanying with a saturation process. The TPA coefficient is measured to be about 211.5  $\text{cm/MW}$  for a  $(\text{PEA})_2\text{PbI}_4$  flake, which is several times/orders of magnitude larger than those of the other semiconductor nanostructures. The giant TPA of 2D perovskite is attributed to the enhanced quantum and dielectric confinements of the inherent multi-quantum-well structure. In addition, the TPA coefficient is demonstrated to be significantly decreased as the sample thickness increases. In the future work, further studies will take advantages of the great nonlinear optical response of the 2D perovskites and focus on development of functional optoelectronic devices for practical applications, such as nonlinear optical modulators and low-threshold multiphoton pumped nanolasers.

### **Supporting Information**

Supporting Information is available online from the Wiley Online Library or from the author.

### **Acknowledgements**

Q. Xiong acknowledges financial support from Singapore National Foundation via an Investigatorship Award (NRF-NRFI2015-03) and a Competitive Research Program (NRF-

Submitted to

CRP-6-2010-2), and Singapore Ministry of Education through AcRF Tier2 grants (MOE2011-T2-2-051 and MOE2015-T2-1-047). P. Lu acknowledges financial support from National Basic Research Program of China (973 Program, No. 2014CB921301). W. Liu would like to acknowledge the scholarship support from Huazhong University of Science and Technology and China Scholarship Council (CSC, No. 201506160035). W. Liu and J. Xing contributed equally to this work.

Received: ((will be filled in by the editorial staff))

Revised: ((will be filled in by the editorial staff))

Published online: ((will be filled in by the editorial staff))

- [1] T. M. Brenner, D. A. Egger, L. Kronik, G. Hodes, D. Cahen, Nat. Rev. Mat. 2016, 1, 15007.
- [2] S. D. Stranks, H. J. Snaith, Nat. Nanotechnol. 2015, 10, 391.
- [3] G. C. Xing, N. Mathews, S. S. Lim, N. Yantara, X. F. Liu, D. Sabba, M. Gratzel, S. Mhaisalkar, T. C. Sum, Nat. Mater. 2014, 13, 476.
- [4] D. Shi, V. Adinolfi, R. Comin, M. J. Yuan, E. Alarousu, A. Buin, Y. Chen, S. Hoogland, A. Rothenberger, K. Katsiev, Y. Losovyj, X. Zhang, P. A. Dowben, O. F. Mohammed, E. H. Sargent, O. M. Bakr, Science 2015, 347, 519.
- [5] M. A. Green, A. Ho-Baillie, H. J. Snaith, Nat. Photonics 2014, 8, 506.
- [6] W. S. Yang, J. H. Noh, N. J. Jeon, Y. C. Kim, S. Ryu, J. Seo, S. I. Seok, Science 2015, 348, 1234.
- [7] H. C. Cho, S. H. Jeong, M. H. Park, Y. H. Kim, C. Wolf, C. L. Lee, J. H. Heo, A. Sadhanala, N. Myoung, S. Yoo, S. H. Im, R. H. Friend, T. W. Lee, Science 2015, 350, 1222.
- [8] J. Xing, F. Yan, Y. Zhao, S. Chen, H. Yu, Q. Zhang, R. Zeng, H. V. Demir, X. Sun, A. Huan, Q. Xiong, ACS Nano 2016, 10, 6623.
- [9] H. M. Zhu, Y. P. Fu, F. Meng, X. X. Wu, Z. Z. Gong, Q. Ding, M. V. Gustafsson, M. T. Trinh, S. Jin, X. Y. Zhu, Nat. Mater. 2015, 14, 636.
- [10] J. Xing, X. F. Liu, Q. Zhang, S. T. Ha, Y. W. Yuan, C. Shen, T. C. Sum, Q. H. Xiong, Nano Lett. 2015, 15, 4571.

- [11] S. T. Ha, C. Shen, J. Zhang, Q. H. Xiong, Nat. Photonics 2016, 10, 115.
- [12] L. T. Dou, A. B. Wong, Y. Yu, M. L. Lai, N. Kornienko, S. W. Eaton, A. Fu, C. G. Bischak, J. Ma, T. N. Ding, N. S. Ginsberg, L. W. Wang, A. P. Alivisatos, P. D. Yang, Science 2015, 349, 1518.
- [13] D. Giovanni, W. K. Chong, H. A. Dewi, K. Thirumal, I. Neogi, R. Ramesh, S. Mhaisalkar, N. Mathews, T. C. Sum, Sci. Adv. 2016, 2, e1600477.
- [14] G. Lanty, A. Brehier, R. Parashkov, J. S. Lauret, E. Deleporte, New J. Phys. 2008, 10, 065007.
- [15] Q. Zhang, R. Su, X. Liu, J. Xing, T. C. Sum, Q. Xiong, Adv. Funct. Mater. 2016, 26, 6238.
- [16] J. Byun, H. Cho, C. Wolf, M. Jang, A. Sadhanala, R. H. Friend, H. Yang, T.-W. Lee, Adv. Mater. 2016, 28, 7515.
- [17] M. Mascheck, S. Schmidt, M. Silies, T. Yatsui, K. Kitamura, M. Ohtsu, D. Leipold, E. Runge, C. Lienau, Nat. Photonics 2012, 6, 293.
- [18] G. Y. Li, C. M. de Sterke, S. Palomba, Laser Photon. Rev. 2016, 10, 639.
- [19] X. Han, K. Wang, H. Long, H. Hu, J. Chen, B. Wang, P. Lu, ACS Photonics 2016, 3, 1308.
- [20] R. Scott, A. W. Achtstein, A. Prudnikau, A. Antanovich, S. Christodoulou, I. Moreels, M. Artemyev, U. Woggon, Nano Lett. 2015, 15, 4985.
- [21] Q. L. Bao, H. Zhang, Z. H. Ni, Y. Wang, L. Polavarapu, Z. X. Shen, Q. H. Xu, D. Y. Tang, K. P. Loh, Nano Res. 2011, 4, 297.
- [22] S. X. Wang, Y. X. Zhang, R. Zhang, H. H. Yu, H. J. Zhang, Q. H. Xiong, Adv. Opt. Mater. 2015, 3, 1342.
- [23] S. Kawata, H. B. Sun, T. Tanaka, K. Takada, Nature 2001, 412, 697.
- [24] G. Walters, B. R. Sutherland, S. Hoogland, D. Shi, R. Comin, D. P. Sellan, O. M. Bakr,

E. H. Sargent, ACS Nano 2015, 9, 9340.

[25] R. Zhang, J. Fan, X. Zhang, H. Yu, H. Zhang, Y. Mai, T. Xu, J. Wang, H. J. Snaith, ACS Photonics 2016, 3, 371.

[26] W.-G. Lu, C. Chen, D. Han, L. Yao, J. Han, H. Zhong, Y. Wang, Adv. Opt. Mater. 2016, 4, 1732.

[27] K. Wang, J. Zhou, L. Yuan, Y. Tao, J. Chen, P. Lu, Z. L. Wang, Nano Lett. 2012, 12, 833.

[28] E. W. Van Stryland, H. Vanherzeele, M. A. Woodall, M. J. Soileau, A. L. Smirl, S. Guha, T. F. Boggess, Opt. Eng. 1985, 24, 244613.

[29] Y. X. Li, N. N. Dong, S. F. Zhang, X. Y. Zhang, Y. Y. Feng, K. P. Wang, L. Zhang, J. Wang, Laser Photon. Rev. 2015, 9, 427.

[30] Y. Wang, X. M. Li, X. Zhao, L. Xiao, H. B. Zeng, H. D. Sun, Nano Lett. 2016, 16, 448.

[31] E. V. Chelnokov, N. Bityurin, I. Ozerov, W. Marine, Appl. Phys. Lett. 2006, 89, 171119.

[32] J. He, J. Mi, H. P. Li, W. Ji, J. Phys. Chem. B 2005, 109, 19184.

[33] S. F. Zhang, N. N. Dong, N. McEvoy, M. O'Brien, S. Winters, N. C. Berner, C. Yim, Y. X. Li, X. Y. Zhang, Z. H. Chen, L. Zhang, G. S. Duesberg, J. Wang, ACS Nano 2015, 9, 7142.

[34] J. Even, L. Pedesseau, C. Katan, Chem. Phys. Chem. 2014, 15, 3733.

[35] Z. Y. Cheng, J. Lin, Crystengcomm 2010, 12, 2646.

[36] T. Ishihara, J. Takahashi, T. Goto, Phys. Rev. B 1990, 42, 11099.

[37] T. Takagahara, E. Hanamura, Phys. Rev. Lett. 1986, 56, 2533.

[38] A. Brehier, R. Parashkov, J. S. Lauret, E. Deleporte, Appl. Phys. Lett. 2006, 89, 171110.

[39] R. Houdré, R. P. Stanley, U. Oesterle, M. Illegems, C. Weisbuch, Phys. Rev. B 1994, 49, 16761.

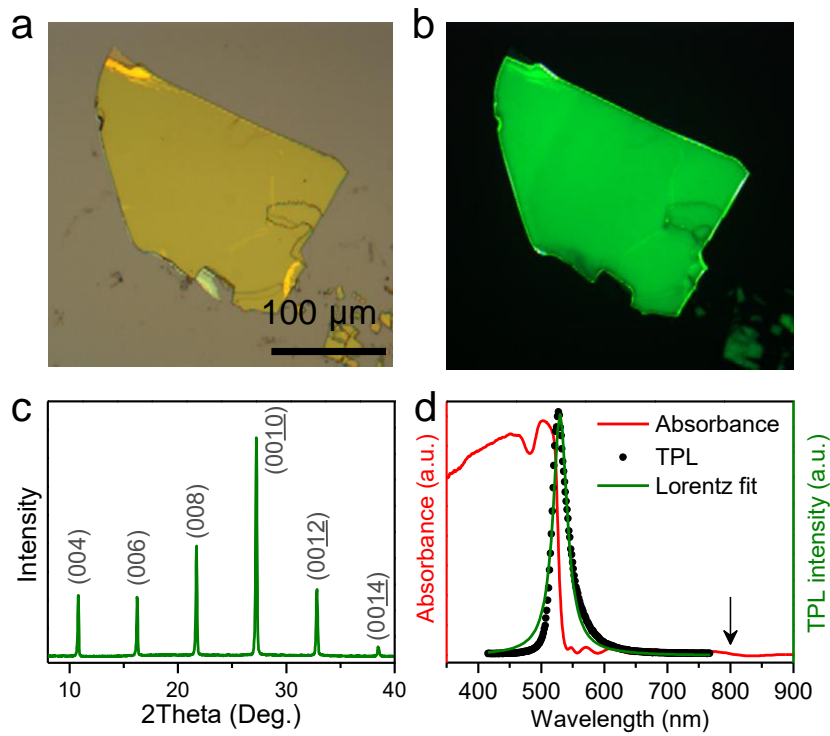


**Figure 1.** (a) Optical microscope image and (b) fluorescence microscope image of a  $(\text{PEA})_2\text{PbI}_4$  flake. (c) XRD pattern of a  $(\text{PEA})_2\text{PbI}_4$  bulk crystal. (d) Linear absorption and TPL spectra of the  $(\text{PEA})_2\text{PbI}_4$  flake. The TPL spectrum was measured under 800 nm femtosecond laser excitation.

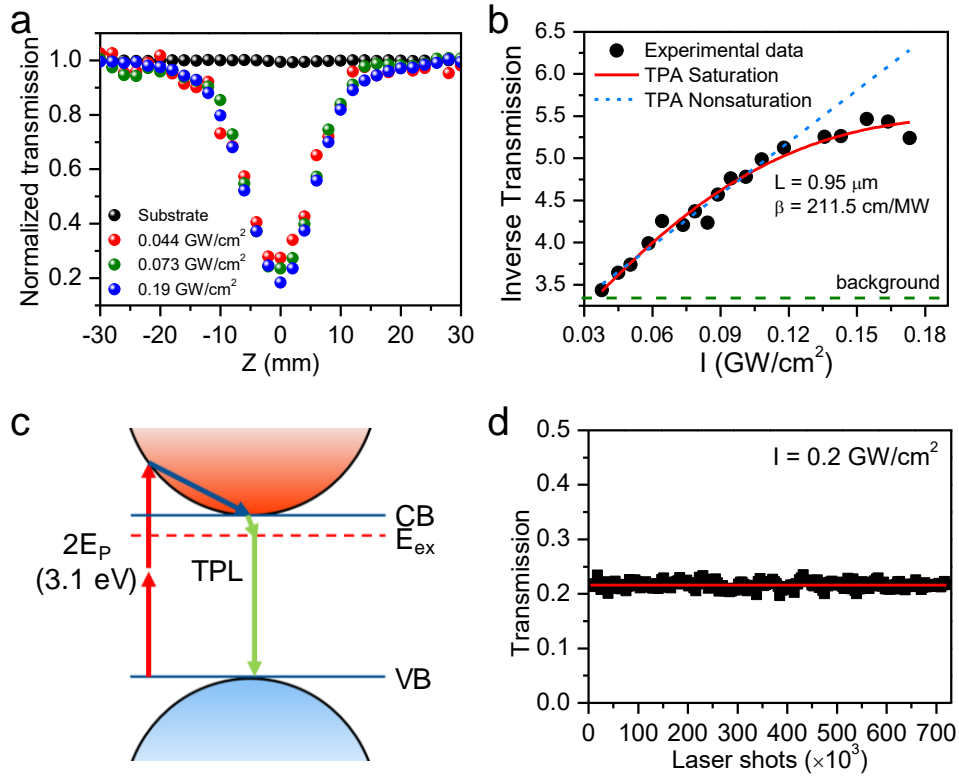


**Figure 2.** (a) Measured OA Z-scan results of a (PEA)<sub>2</sub>PbI<sub>4</sub> flake at different peak intensities. (b) Inverse transmission as a function of peak intensity for the (PEA)<sub>2</sub>PbI<sub>4</sub> flake, fitted by TPA saturation (red curve) and nonsaturation (blue dashed line) models respectively. The green dashed line indicates a background (linear transmission) containing linear reflection and scattering. (c) Schematic of TPA and TPL process. (d) Normalized transmission as a function of laser shots by keeping the (PEA)<sub>2</sub>PbI<sub>4</sub> flake at the laser beam waist.

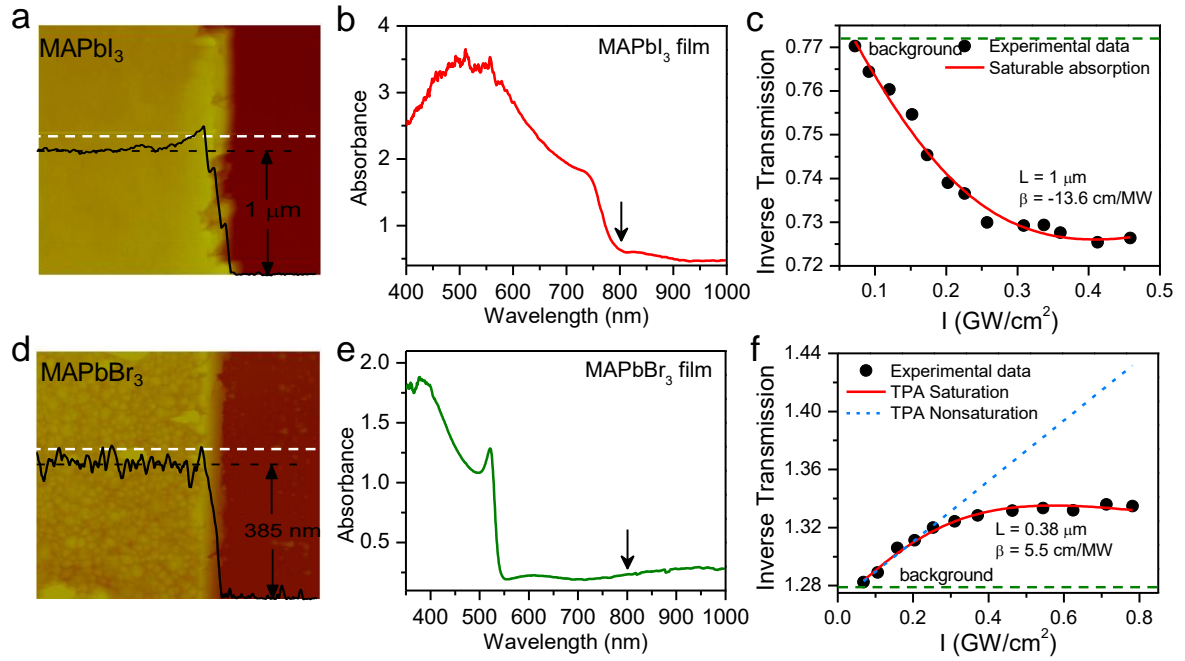


**Figure 3.** (a) Atomic force microscope (AFM) pattern of a MAPbI<sub>3</sub> film. (b) Linear absorption spectrum of the MAPbI<sub>3</sub> film. (c) Plot of inverse transmission *versus* incident intensity for the MAPbI<sub>3</sub> film. (d) Atomic force microscope (AFM) pattern of a MAPbBr<sub>3</sub> film. (e) Linear absorption spectrum of the MAPbBr<sub>3</sub> film. (f) Plot of inverse transmission *versus* incident intensity for the MAPbBr<sub>3</sub> film.

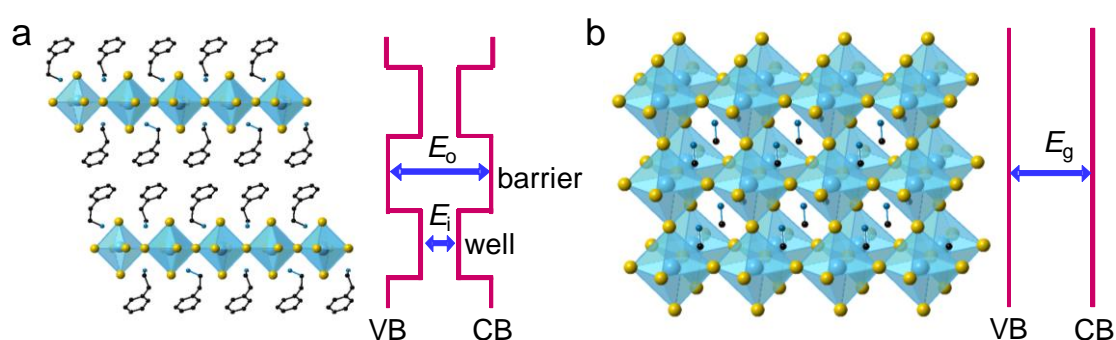


**Figure 4.** Schematics of crystalline structure and electric structure for (a) 2D and (b) 3D perovskites. Yellow ball: X (X = I, Br); blue ball: Pb; black chain: organic molecules.  $E_o$  and  $E_i$  indicate the bandgaps of organic layer (barrier) and inorganic layer (well) respectively, and  $E_g$  denotes the bandgap of 3D perovskite.

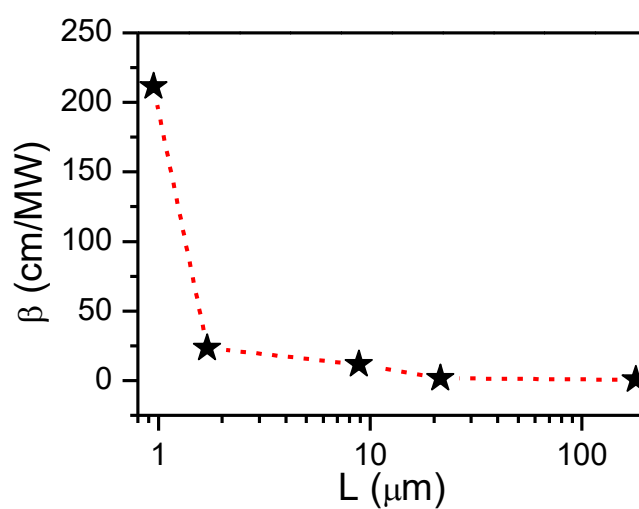


**Figure 5.** Plot of TPA coefficient *versus* sample thickness for the  $(\text{PEA})_2\text{PbI}_4$  flake.

**Table 1.** Nonlinear absorption parameters for different nanostructures at 800 nm

Material	Bandgap (eV)	Thickness	Nonlinear absorption	$\beta$ (cm/MW)	$I_{\text{sat}}$ (GW/cm <sup>2</sup> )
ZnO nanoparticles <sup>[31]</sup>	3.37	5-10 nm	TPA <sup>a)</sup>	0.11	N/A
CdS nanocrystals <sup>[32]</sup>	2.71	1.8 $\mu\text{m}$	TPA	0.011	190
WS <sub>2</sub> monolayer <sup>[33]</sup>	1.95	0.75 nm	TPA	0.525	N/A
WS <sub>2</sub> few-layer <sup>[33]</sup>	indirect	15 nm	SA <sup>b)</sup>	-0.4	N/A
MAPbI <sub>3</sub> film	1.61	1 $\mu\text{m}$	SA	-13.6	N/A
MAPbBr <sub>3</sub> film	2.21	0.38 $\mu\text{m}$	SA, TPA	5.5	0.57
(PEA) <sub>2</sub> PbI <sub>4</sub> flake	2.4	0.95 $\mu\text{m}$	TPA	211.5	0.21
(PEA) <sub>2</sub> PbI <sub>4</sub> film	2.4	1.94 $\mu\text{m}$	TPA	12.6	0.22

<sup>a)</sup>TPA-two-photon absorption; <sup>b)</sup>SA-saturable absorption.

### The table of contents entry

Two-dimensional (2D) organic-inorganic perovskite, composed of alternative organic and inorganic layers, exhibits a giant two-photon absorption (TPA) effect. The TPA coefficient of a (PEA)<sub>2</sub>PbI<sub>4</sub> flake is measured to be 211.5 cm/MW at 800 nm. The large TPA can be attributed to enhanced quantum and dielectric confinement in the organic-inorganic multi-quantum-well structure.

### Keywords

2D organic-inorganic perovskite; multi-quantum-well structure; nonlinear optics; optoelectronic devices; two-photon absorption

Weiwei Liu, Jun Xing, Jiabin Zhao, Xinglin Wen, Kai Wang, Peixiang Lu,\* and Qihua

Xiong\*

### Title

Giant Two-photon Absorption and Its Saturation in Two-dimensional Organic-inorganic Perovskite

### ToC figure

